

# Separation of Intramembrane Charging Components in Low-Calcium Solutions in Frog Skeletal Muscle

CHRISTOPHER L.-H. HUANG

From the Physiological Laboratory, Cambridge CB2 3EG, United Kingdom

**ABSTRACT** The inactivation of charge movement components by small ( $-100$  to  $-70$  mV) shifts in holding potential was examined in voltage-clamped intact amphibian muscle fibers in low  $[Ca^{2+}]$ ,  $Mg^{2+}$ -containing solutions. The pulse protocols used both large voltage excursions and smaller potential steps that elicited prolonged ( $q_r$ ) transients. Charge species were distinguished through the pharmacological effects of tetracaine. These procedures confirmed earlier observations in cut fibers and identified the following new properties of the  $q_r$  charge. First,  $q_r$ , previously defined as the tetracaine-sensitive charge, is also the component primarily responsible for the voltage-dependent inactivation induced by conditions of low extracellular  $[Ca^{2+}]$ . Second, this inactivation separates a transient that includes a "hump" component and which has kinetics and a voltage dependence distinct from the monotonic decay that remains. Third,  $q_r$ , previously associated with delayed charge movements, can also contribute significant charge transfer at early times. These findings suggest that the parallel inhibition of calcium signals and charge movements reported in low  $[Ca^{2+}]$  solutions arises from influences on  $q_r$  charge (Brum et al., 1988*a, b*). They also reconcile reports that implicate tetracaine-sensitive ( $q_r$ ) charge in excitation-contraction coupling with evidence that early intramembrane events are also involved in this process (Pizarro et al., 1989). Finally, they are relevant to hypotheses of possible feedback or feed-forward roles of  $q_r$  in excitation-contraction coupling.

## INTRODUCTION

There has been increasing evidence that a number of different components of capacitative charge reside in the membrane of skeletal muscle. One approach separated the transfers of  $q_b$  and  $q_r$  components when depolarizing steps were applied to fully polarized muscle fibers. The  $q_r$  component has been identified through its tetracaine susceptibility. It is also associated with the slow charging currents observed near the contractile threshold in intact muscle fibers (Adrian and Peres, 1979; Huang, 1981; Hui, 1983; Adrian and Huang, 1984*a*; Hui and Chandler, 1990). Detubulation studies localized it to membranes of the transverse tubular

Address reprint requests to Dr. C. L.-H. Huang, Physiological Laboratory, Downing Street, Cambridge CB2 3EG, UK.

system. The remaining  $q_{\beta}$  charge appeared to have a less selective distribution over both surface and tubular membranes (Huang and Peachey, 1989).

A range of parallels exists between properties of  $q_{\gamma}$  charge and the regulation of excitation–contraction coupling. The appearance of  $q_{\gamma}$  currents coincided with the onset of contractile activation and of threshold cytosolic  $Ca^{2+}$  signals (see Huang, 1988, for a review). There are also pharmacological similarities concerning the effects of tetracaine (Huang, 1981, 1983; Vergara and Caputo, 1982; Hui, 1983). Charge inactivation was accompanied by reductions in intracellular calcium signals in partially depolarized cut fibers treated with nifedipine (Rios and Brum, 1987). This finding was corroborated in intact fibers. The immobilized charge fell within the category of tetracaine-sensitive  $q_{\gamma}$ , as opposed to  $q_{\beta}$  charge (Huang, 1990).

A further concordance between charge inactivation and the inhibition of excitation–contraction coupling was observed in cut fibers studied in EGTA-containing solutions. The extracellular  $Ca^{2+}$  was replaced by  $Mg^{2+}$  (Brum et al., 1988*a, b*). Small shifts in holding potential then partially immobilized the nonlinear charge. There was a coincident inhibition of  $Ca^{2+}$  release in response to depolarizing steps. However, this report did not examine the fate of individual capacity components. Instead, the entire charge moved with depolarizing voltages was examined as charge I (Schneider and Chandler, 1973; Adrian and Almers, 1976*a, b*).

This paper applies such solution changes to intact as opposed to cut fibers. Confirmation of findings in both preparations is important in view of differences in results that arise from intact and cut fibers (see Chandler and Hui, 1990, for a discussion). The findings are then traced to influences on individual charge species; this was not attempted in the earlier study. Both its pharmacological properties and its association with delayed currents at some potentials were used as criteria to distinguish the  $q_{\gamma}$  component. Finally, the preferential inactivation of charge was developed into a means of separating  $q_{\beta}$  and  $q_{\gamma}$  transients.

#### METHODS

Frog (*Rana temporaria*) sartorius muscles were dissected in cooled Ringer solution at 4°C and mounted in a temperature-controlled recording chamber. Each muscle was stretched to give fibers with a center sarcomere length of 2.2–2.4  $\mu\text{m}$ . This was measured using an eyepiece graticule with a Zeiss Oberkochen  $\times 40$  water immersion objective. The bathing solution was then altered to a hypertonic tetraethylammonium-containing solution (see below). Studies were made at 3.5–4.2°C. The pelvic ends of the superficial muscle fibers directly accessible to the bathing solution were subject to a three-microelectrode voltage clamp (Adrian and Almers, 1976*a, b*; Adrian, 1978; Adrian and Rakowski, 1978). This used conventional glass microelectrodes of resistance 4–10 M $\Omega$ . These were positioned at distances of  $l = 375 \mu\text{m}$  (voltage control electrode,  $V_1$ ),  $2l = 750 \mu\text{m}$  (second voltage electrode,  $V_2$ ), and  $5l/2 = 875 \mu\text{m}$  (current injection electrode,  $I_0$ ), respectively, from the pelvic end of the fiber. The voltage recording electrodes contained 3 M KCl, and the current injection electrode contained 2 M K citrate.

Values of linear cable constants were calculated from the steady values of  $V_1(t)$ ,  $V_2(t)$ , and the injected current,  $I_0(t)$ , at the end of the 20-mV control steps. These were imposed 500 ms after the fiber was subjected to a prepulse level of  $-120$  mV, from a holding voltage of  $-100$  mV. They gave values of the length constant,  $\lambda$ , internal longitudinal resistance,  $r_i$ , and membrane resistance of unit fiber length,  $R_m$ . The fiber diameter,  $d$ , and specific membrane resistance,  $R_m$ , were then calculated. This assumed a value of the internal sarcoplasmic resistivity,  $R_p$ , of 391

ohm.cm in 2.5 times hypertonic solution at 2°C, with a  $Q_{10}$  of 0.73 (Hodgkin and Nakajima, 1972). The membrane current through unit area of fiber surface,  $I_m(t)$ , was computed as:

$$I_m(t) = [V_1(t) - V_2(t)]d/(6l^2R_i)$$

where  $t$  is time.

Leak admittances were determined from the baseline currents left after the capacity decays. A best-fit straight line was obtained and the fitted pedestal was subtracted from the record. It was only very rarely necessary to use a sloping baseline for this subtraction (see Huang and Peachey, 1989). The capacitive charge moved by the applied voltage step,  $\Delta V_1(t)$ , was determined by integration of the on and off transients of the resulting record using Simpson's rule (Adrian and Almers, 1974; Chandler et al., 1976; Adrian, 1978):

$$Q = \int [I_m(t) - (1/R_m) \Delta V_1(t)]dt$$

On and off integrals were compared to check for charge conservation. Their mean values and computed values of the linear cable constants were then used to calculate the effective linear electrical capacity. This was referred to unit apparent lateral fiber surface area (in  $\mu\text{F}/\text{cm}^2$ ). Control records were compared with currents obtained in the test pulse procedures, described individually in the Results. The control transients were first scaled by the relative magnitudes of the applied test and control voltage steps. The resulting arrays were then subtracted from the test transients to derive the nonlinear charge movement.

The above numerical procedures were performed on records of  $V_1(t)$ ,  $V_1(t) - V_2(t)$ , and  $I_0(t)$ . These were obtained at a 12-bit analog-to-digital conversion interval of 200  $\mu\text{s}$ . The originating signals were filtered through 3-pole Butterworth filters set to a cut-off frequency of 1 kHz. They were sampled using a PDP 11/23 computer (Digital Equipment Corp., Maynard, MA) with a model 502 interface (Cambridge Electronic Design, Cambridge, UK). Five sweeps were averaged in each test or control record when measuring steady-state charge. However, in experiments that studied the transients attributed to different species of nonlinear charge, each record was the average of 10 sweeps. Sets of five determinations of test charge were bracketed by the control protocol. This precaution additionally enabled fiber stability and condition to be monitored.

Electrical recordings were made at 3–4°C in either of two bathing solutions. Both of these represent modifications from solutions adopted in earlier work. The control solution consisted of 80 mM tetraethylammonium sulphate, 15 mM tetraethylammonium chloride, 2.5 mM  $\text{Rb}_2\text{SO}_4$ , 8 mM  $\text{CaSO}_4$ , 350 mM sucrose, and 3 mM *N*-2-hydroxyethylpiperazine-*N'*-2-ethanesulfonic acid (HEPES). It was buffered to pH 7.0 (cf. Adrian and Peres, 1979; Huang, 1982). The test solution replaced the  $\text{CaSO}_4$  with 3 mM  $\text{MgSO}_4$  and 1.22 mM ethyleneglycol-bis-( $\beta$ -aminoethylether)-*N,N'*-tetraacetic acid (EGTA). The latter accordingly resembled the solutions introduced in earlier studies of  $\text{Ca}^{2+}$  deprivation (Brum et al., 1988a, b). Studies were made in the absence or presence of 1 mM tetracaine. All experiments were performed within 1 h of introducing either test or control solutions.

$\text{Ca}^{2+}$  activities were assessed in all the solutions used. A  $\text{Ca}^{2+}$ -selective electrode (model ISE-310; E.D.T. Analytical plc, Uxbridge, UK) was referenced against a saturated calomel reference electrode placed in the same solution. Potentials were read from an expanded range high impedance digital millivoltmeter (Dow-Corning, Halstead, UK). As sulfate was used as anion, results were expressed in terms of  $\text{Ca}^{2+}$  activities rather than concentrations. Standard solutions with known  $\text{Ca}^{2+}$  concentrations and ionic strengths were used to calibrate the electrodes. The  $\text{Ca}^{2+}$  activities were then deduced from these concentrations through the use of reference curves that were provided for the standard calibrating solutions. These related activity coefficient to ionic strength. The experimental solutions that contained normal [ $\text{Ca}^{2+}$ ]

had  $\text{Ca}^{2+}$  activities around 1.4 mM. Activities fell below 1  $\mu\text{M}$  in the EGTA-containing solutions. The latter was a limiting figure obtained using an empirical calibration that extended one order of magnitude below the observed linear detection limit of the  $\text{Ca}^{2+}$ -sensitive electrode. Finally, a dissociation constant between EGTA and  $\text{Mg}^{2+}$  of  $2.47 \times 10^{-2}$  M was assumed. Using an [EGTA] of 1.22 mM, this gave a free [ $\text{Mg}^{2+}$ ] of 2.87 mM in the low [ $\text{Ca}^{2+}$ ] solution (Sillen and Martell, 1971; Brum et al., 1988a).

## RESULTS

### *Control Membrane Capacitances*

Two types of experiments were performed. First, the voltage-dependent inactivation induced by low [ $\text{Ca}^{2+}$ ] solutions was investigated in the steady state. Second, the kinetic properties of the charge responsible were explored. The former studies imposed large test steps of fixed amplitude between  $-100$  and  $-20$  mV. These were applied 500 ms after a prepulse to a conditioning voltage of  $-100$  mV. Thus, only the holding potential was varied, and this particularly through small potential displacements in 10-mV increments, between  $-100$  and  $-60$  mV. The test pulses were imposed at least 30 s after each shift in holding voltage (cf. Brum et al., 1988a).

Particular precautions were included to ensure consistent control records with which test findings could be compared. First, it was necessary to allow for, or ensure the reversal of, any charge interconversion that might accompany changes in holding conditions. Experiments always began at a holding potential of  $-100$  mV. The linear membrane and cable constants were determined by the use of 20-mV depolarizing control steps of 124-ms duration. These were imposed 500 ms after the onset of a  $-120$ -mV conditioning potential. Such control protocols were repeated to bracket successive experimental runs. They were always performed with the holding potential returned to  $-100$  mV, whatever the holding voltages explored in the test pulses. This bracketing procedure ensured constant control pulse conditions, and avoided discrepancies from charge interconversions consequent upon holding potential (Brum and Rios, 1987).

Second, cable constants calculated from the successive bracketing control records were scrutinized for systematic changes in the course of each experiment. The capacitances at the end of each experiment were compared with those obtained at the outset, before holding voltage was altered. The following ratios were obtained in the fibers in the different solutions: (a) normal  $\text{Ca}^{2+}$ , 0 tetracaine:  $1.04 \pm 0.036$  (mean  $\pm$  SEM, six fibers); (b) low  $\text{Ca}^{2+}$ , 0 tetracaine:  $1.027 \pm 0.035$  (five fibers); (c) normal  $\text{Ca}^{2+}$ , 1 mM tetracaine:  $1.074 \pm 0.022$  (five fibers); and (d) low  $\text{Ca}^{2+}$ , 1 mM tetracaine:  $1.024 \pm 0.014$  (six fibers). Thus, there was no significant change ( $P > 5\%$  on *t*-testing) in the values of control capacitance through the experiments discussed here.

Third, charge interconversion could potentially arise from the ionic manipulations themselves. These would cause altered but otherwise stable values of the control capacitance. However, the sizes of both the test and control steps were fixed. The subtraction to obtain nonlinear charge accordingly involved a consistent amount of control charge scaled by a fixed ratio of test to control voltage excursions, whatever

the holding voltage. At the very least, therefore, the findings below correctly represent any changes in the charge available within any given group of fibers.

*Effects of  $\text{Ca}^{2+}$  on Inactivation of Steady-State Components*

Fig. 1, A–D, plots the alterations in charge moved by voltage steps from  $-100$  to  $-20$  mV (mean  $\pm$  SEM) against holding potential,  $V_H$ , in the different external solutions. The comparisons primarily concern alterations in the available charge, rather than

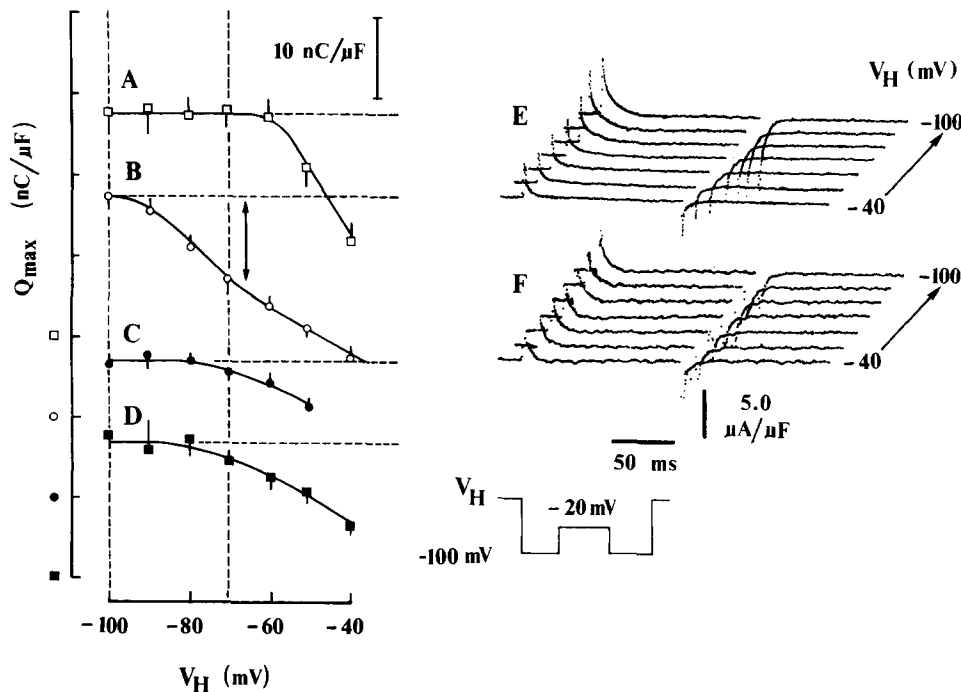


FIGURE 1. Steady-state charge (means  $\pm$  SEM) moved by voltage steps between a  $-100$ -mV prepulse potential and a fixed test voltage of  $-20$  mV (see inset), plotted against the holding potential,  $V_H$ . Plots of steady-state charge in this and subsequent figures are means of on and off charge movement. Lines were drawn by eye. (A) Fibers in control  $[\text{Ca}^{2+}]$  with tetracaine absent (six fibers;  $d = 79.7 \pm 6.56 \mu\text{m}$ ,  $R_m = 16.04 \pm 3.98 \text{ k}\Omega \text{ cm}^2$ ,  $C_m = 11.76 \pm 1.59 \mu\text{F}/\text{cm}^2$ ). (B) Fibers in EGTA-containing low  $[\text{Ca}^{2+}]$  solutions in the absence of tetracaine (six fibers;  $d = 80.1 \pm 5.76 \mu\text{m}$ ,  $R_m = 7.54 \pm 2.04 \text{ k}\Omega \text{ cm}^2$ ,  $C_m = 10.7 \pm 1.44 \mu\text{F}/\text{cm}^2$ ). Partial charge inactivation marked by arrowheads. (C) Fibers in low  $[\text{Ca}^{2+}]$  in EGTA-containing solutions in the presence of  $1 \text{ mM}$  tetracaine (six fibers;  $d = 67.92 \pm 5.066 \mu\text{m}$ ,  $R_m = 6.37 \pm 1.85 \text{ k}\Omega \text{ cm}^2$ ,  $C_m = 6.38 \pm 0.48 \mu\text{F}/\text{cm}^2$ ). (D) Fibers in control extracellular  $[\text{Ca}^{2+}]$  and  $1 \text{ mM}$  tetracaine (four fibers;  $d = 54.5 \pm 6.22 \mu\text{m}$ ;  $R_m = 12.31 \pm 2.48 \text{ k}\Omega \text{ cm}^2$ ,  $C_m = 6.04 \pm 0.71 \mu\text{F}/\text{cm}^2$ ). Cable constants given as means  $\pm$  SEM. (E and F) Charge movements obtained from fibers in the absence (E) and presence (F) of tetracaine at a range of holding potentials,  $V_H$ , under conditions of low extracellular  $[\text{Ca}^{2+}]$ . Specific cable constants from control steps: fiber R06 (E),  $d = 60.7 \mu\text{m}$ ,  $R_m = 4.7 \text{ k}\Omega \text{ cm}^2$ ,  $C_m = 7.2 \mu\text{F}/\text{cm}^2$ . Fiber R13 (F),  $d = 63.0 \mu\text{m}$ ,  $R_m = 4.4 \text{ k}\Omega \text{ cm}^2$ ,  $C_m = 9.6 \mu\text{F}/\text{cm}^2$ .

absolute quantities. The data are therefore plotted on separate ordinates, with the dotted lines indicating zero alteration for each group of points. The value for zero charge is marked along the ordinate with the corresponding symbol for that group of points.

In normal extracellular  $[Ca^{2+}]$ , a change in holding voltage from  $-100$  to  $-70$  mV did not significantly alter the charge movement if tetracaine was absent. This quantity remained close to  $28$  nC/ $\mu$ F (Fig. 1 *A*), in agreement with earlier reports in intact fibers (e.g., Huang, 1982; Hui, 1983). Cut fibers had differing features in this respect, showing some inactivation even at these holding levels (Brum et al., 1988*a*). However, significant inactivation was observed with larger depolarizations positive to  $-60$  mV in the intact fibers. For example, a holding voltage of  $-40$  mV removed  $>15$  nC/ $\mu$ F of the charge (Fig. 1 *A*). However, tetracaine-resistant ( $q_{\beta}$ ) charge was then also significantly inactivated (Fig. 1 *D*). This precluded a straightforward separation of the contributing components in solutions with normal  $[Ca^{2+}]$ .

In reduced extracellular  $[Ca^{2+}]$ , even small holding potential shifts caused noticeable charge inactivation in the intact fibers. In fully polarized fibers charge movement was similar in both solutions. However, a shift in holding potential from  $-100$  to  $-70$  mV now reduced the overall charge by  $\sim 10$  nC/ $\mu$ F (Fig. 1 *B*, *arrow*). The addition of  $1.0$  mM tetracaine reduced the charge movement even in fully polarized fibers. It left similar amounts of charge,  $\sim 17$  nC/ $\mu$ F, whether extracellular  $Ca^{2+}$  was reduced (Fig. 1 *C*) or normal (Fig. 1 *D*). However, shifts in holding voltage between  $-100$  and  $-70$  mV now produced relatively little further immobilization ( $1.1$ – $1.7$  nC/ $\mu$ F) and gave similar inactivation functions in both conditions of external  $[Ca^{2+}]$ .

These steady-state results confirm for intact fibers the voltage-dependent charge inactivation in low  $[Ca^{2+}]$  reported in cut fibers. They also implicate the  $q_{\gamma}$  species, identified through its sensitivity to tetracaine, in this effect. In contrast, the tetracaine-resistant ( $q_{\beta}$ ) charge did not appear to contribute greatly to this inactivation.

#### *The Influence of Holding Voltage on Charging Kinetics*

The above experiments analyzed charge inactivation on the basis of steady-state pharmacological properties. The  $q_{\beta}$  and  $q_{\gamma}$  species also have distinct kinetic properties, but these can be discerned only close to the voltage threshold for contractile activation (Adrian and Peres, 1979; Huang, 1981; Hui, 1983). The charge movements elicited by large depolarizing steps were relatively rapid monotonic decays not amenable to a kinetic separation either before (Fig. 1 *E*) or after (Fig. 1 *F*) addition of tetracaine. Nevertheless, the current records were in accord with the findings in Fig. 1, *A*–*D*. The charge movements diminished even with small holding potential shifts from  $-100$  mV in the absence of tetracaine (*E*). Addition of tetracaine (*F*) reduced their size even in fully polarized fibers. However, small shifts in holding level from  $-100$  mV then produced little further reduction in the currents.

The second type of experiment sought conditions under which the kinetics of  $q_{\beta}$  and  $q_{\gamma}$  charge could be separated. It required smaller voltage clamp steps to elicit slow charge movements. The test steps were applied at a 500-ms interval after a prepulse to a level of  $-100$  mV. First, a range of test voltages was explored with a fixed holding potential of  $-100$  mV, to determine levels at which slow charging transients took place. The test voltage was then fixed to a membrane potential within

this range and test pulses were made with varying holding potentials. Charge movements were derived from a comparison of the resulting test records and the control records obtained at a  $-100$ -mV holding level at the outset of the experiment. It was then possible to investigate whether the time course of the inactivated charge movement was similar to, or was distinct from, the currents that remained.

Fig. 2 illustrates results in one such fiber at which the test steps were made to a fixed level of  $-53$  mV, under conditions of low external  $[Ca^{2+}]$ . Fig. 2A shows the charge movements through holding potentials between  $-100$  and  $-70$  mV. Fig. 2B monitors the changes in the charge movement through these shifts by displaying the differences between each trace (A) with the first record obtained at a holding potential of  $-100$  mV, starting with the trace obtained at  $-90$  mV. Between holding potentials of  $-100$  and  $-80$  mV, these difference traces were flat and so indicated no

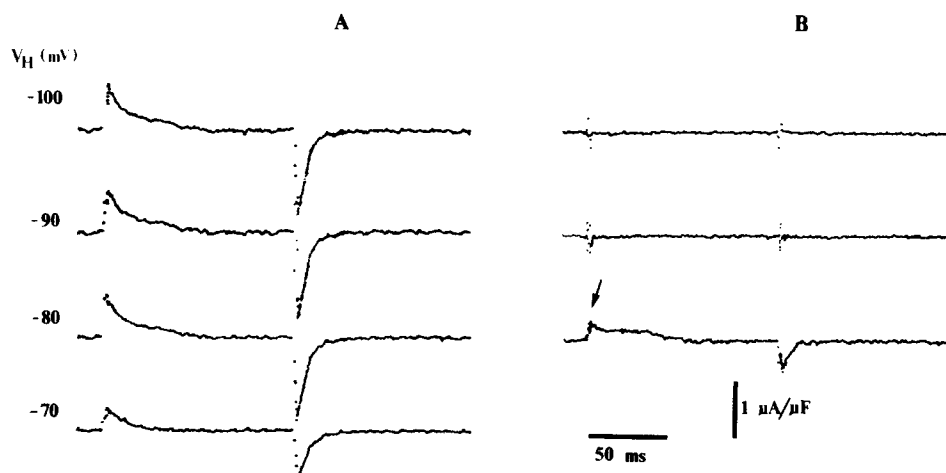


FIGURE 2. (A) Charge movements obtained in response to voltage steps from a prepulse voltage of  $-100$  mV, to a fixed ( $-53$  mV) testing voltage at which slow charging currents occurred in on responses, shown with (B) the difference between each trace, beginning with the record at  $-90$  mV, and the trace obtained at  $-100$  mV. Fiber in low  $[Ca^{2+}]$ , EGTA-containing solution (specific fiber cable constants):  $d = 75.8$   $\mu\text{m}$ ,  $R_m = 9.09$   $\text{k}\Omega \text{ cm}^2$ ,  $C_m = 9.66$   $\mu\text{F/cm}^2$ .

significant inactivation. The records (A) then showed relatively prolonged on currents that extended beyond 50 ms. The "off" tails were initially larger, but decayed more rapidly (10–15 ms). However, a shift of holding voltage from  $-80$  to  $-70$  mV reduced the size of the charge movement. Among individual fibers this reduction took place either between  $-90$  and  $-80$  mV, or between  $-80$  and  $-70$  mV. The subtracted trace (Fig. 2B, arrow) suggested that this inactivation selectively involved delayed portions of the charge movement and not merely a simple scaling down of the waveform as a whole.

#### *Control Transients in Low- $[Ca^{2+}]$ Solutions*

The above studies required consistent control transients from which the nonlinear current could be derived. This point was investigated in the same fibers along the

same lines as in the steady-state studies described above. The controls also examined for effects on the transients as well as the values of steady-state charge. First, the control voltage steps were imposed between potentials of  $-120$  and  $-100$  mV through the holding potential changes between  $-100$  and  $-70$  mV. Fig. 3 displays the resulting capacity currents before (*A*) and after (*B*) the holding voltage was moved from  $-100$  to  $-70$  mV, and after its return to  $-100$  mV (*C*). It also plots differences between successive traces ( $B - A$  and  $C - B$ ), and between the traces before and after holding level was manipulated ( $C - A$ ). Only small alterations in either steady-state

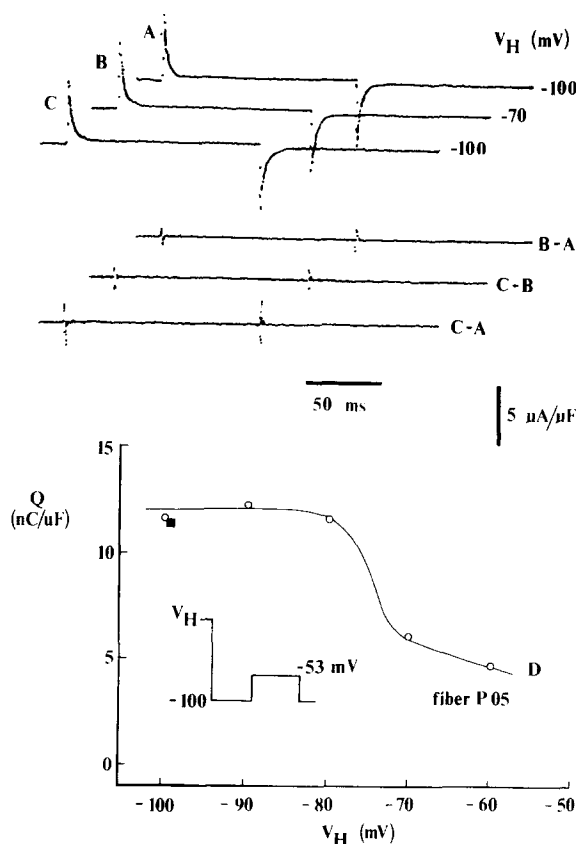


FIGURE 3. (*Top*) Capacity transients elicited by control steps (*inset*) before (*A*), during (*B*), and after (*C*) changes in holding potential from  $-100$  to  $-70$  mV, shown with the subtractions  $B - A$ ,  $C - B$ , and  $C - A$ . (*Bottom*) Steady-state nonlinear charge movement,  $Q$ , plotted against holding voltage  $V_H$  (*D*; circles). The line was drawn by eye. The filled square denotes a repeat measurement made after returning the holding voltage to  $-100$  mV. Same fiber as in Fig. 2. Measurements of cable constants (*A*) immediately before change in holding voltage,  $R_m = 9.12$  k $\Omega$  cm $^2$ ,  $C_m = 10.2$   $\mu F$ /cm $^2$ ; (*B*) at the altered holding potential,  $R_m = 8.27$  k $\Omega$  cm $^2$ ,  $C_m = 10.09$   $\mu F$ /cm $^2$ ; (*C*) after return of the holding potential to  $-100$  mV,  $R_m = 8.3$  k $\Omega$  cm $^2$ ,  $C_m = 10.1$   $\mu F$ /cm $^2$ .

capacitances (Fig. 3, legend) or the charging records were observed. Even then any such differences in the transients occurred only early ( $< 1$  ms) after the steps, and so would not affect the more prolonged nonlinear currents.

Second, the reversibility of any nonlinear changes was verified. The variation of steady-state charge,  $Q$ , moved by the test step with holding potential,  $V_H$  (Fig. 3 *D*) corroborated the charging records in Fig. 2 *A* in that variations in holding potential between  $-100$  and  $-80$  mV did not affect steady-state charge movement. However, further depolarization from  $-80$  to  $-70$  mV (or  $-90$  to  $-80$  mV in some fibers)



caused marked charge inactivation. Nevertheless, this immobilization reversed with a return of the holding level to  $-100$  mV (Fig. 3 *D*, filled symbol).

Finally, one might consider charge interconversions to be due to the ionic manipulations used in the experiments. The control records used to derive all the records of the kind shown in Fig. 2 *A* were obtained at the outset of each experiment. As the test voltage excursion was constant, the subtraction procedure therefore involved a constant control transient scaled by a consistent ratio of test to control voltage steps. This would therefore provide a consistent control subtraction. Furthermore, the inactivated charge movements (e.g., Fig. 2 *B*) were obtained from the test records at the different holding voltages. Their computation thus did not involve the control records. These would therefore not be affected by variations in control capacitance.

#### *Signal Averages of Difference Traces*

A closer examination of the inactivation effect was performed through heavier signal averaging of on records in the same fiber both before and after inactivation, using the

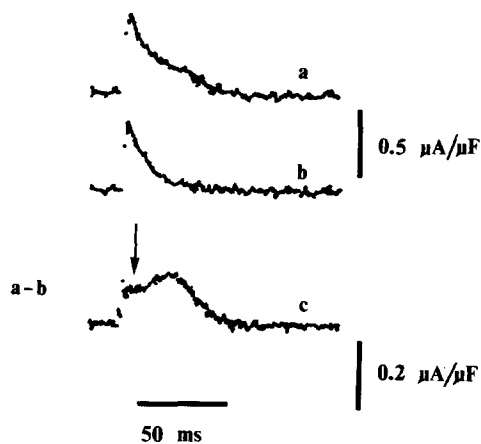


FIGURE 4. Traces obtained in response to test steps after heavier signal averaging (10 sweeps/record) at holding voltages of  $-80$  mV (*a*) and  $-70$  mV (*b*). The charge movement inactivation (*c*), displayed at higher gain, resulted from the shift in holding voltages, and was obtained from the difference between *a* and *b*. Same fiber as in Fig. 2. Early charge transfer in *c* marked by arrow.

same testing voltage (Fig. 4). Transients were obtained at holding voltages of  $-80$  mV (*a*) and  $-70$  mV (*b*) and then compared. These corresponded to the holding values between which most of the inactivation took place (Fig. 3 *D*). The partial inactivation left a more rapid nonlinear decay, which was complete over  $\sim 30$  ms (Fig. 4 *b*). Charge inactivation in low  $[Ca^{2+}]$  solutions therefore does not merely cause a simple scaling-down of the entire charging current. Rather, it appears to involve a kinetically distinct component of the intramembrane charge. Fig. 4 *c* displays, at a higher gain, the inactivated current (*c*) obtained from the difference (*a* - *b*). This record contained the delayed hump component, which extended well over 50 ms, and which was more prominent than in either record *a* or *b*. Finally, the difference current (*c*) showed significant charging current even at early times after the imposition of the voltage step (Fig. 4 *c*, arrow).

*Shifts in Holding Voltage and  $q_{\beta}$  Transients*

Contrasting findings were obtained in the presence of 1 mM tetracaine in experiments in tetracaine-treated fibers at a fixed ( $-40$  mV) test potential (Fig. 5 *A*). This depolarization was close to, but larger than, those used in any of the kinetic studies made when local anaesthetic was absent. They therefore displaced at least as much  $q_{\beta}$  charge as the previous experiments. The holding potential,  $V_H$ , again was varied between  $-100$  and  $-60$  mV. The  $q_{\beta}$  charge movements were exponential in form and lacked distinct slow ( $q_v$ ) charging transients, in agreement with earlier findings (Huang, 1982). Fig. 5 *B* shows a comparison of each record with the transient obtained at a holding potential of  $-100$  mV, beginning with the trace obtained at

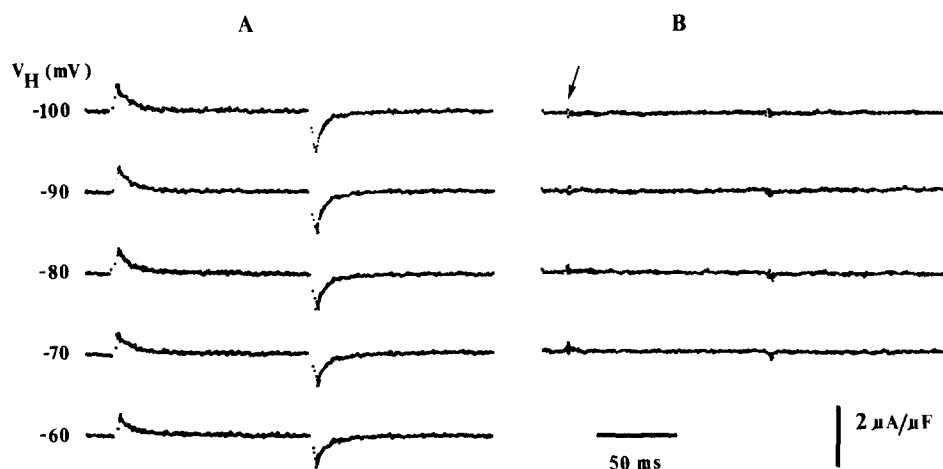


FIGURE 5. (*A*) Charge movements elicited by a fixed voltage step between a conditioning level of  $-100$  mV and a test potential of  $-40$  mV, over a range of holding voltages,  $V_H$ . (*B*) Differences between each trace, beginning with the record at  $-90$  mV, and the trace obtained at  $-100$  mV. Onset of on step marked by arrow. Fiber in EGTA-containing, low  $[Ca^{2+}]$  solution with 1 mM tetracaine:  $d = 78.5$   $\mu\text{m}$ ,  $R_m = 5.65$   $\text{k}\Omega \text{ cm}^2$ ,  $C_m = 5.9$   $\mu\text{F}/\text{cm}^2$ . Charges moved at holding voltages of  $-100$ ,  $-90$ ,  $-80$ ,  $-70$ , and  $-60$  mV were 7.09, 7.15, 7.0, 6.9, and 6.7  $\text{nC}/\mu\text{F}$ , respectively.

$-90$  mV. The flat difference traces indicate little change in charge movement with alterations of holding potential between  $-100$  and  $-60$  mV. In agreement with the steady-state measurements illustrated in Fig. 1, these findings suggest that relatively little of the charge immobilization examined here arises from  $q_{\beta}$  charge.

*Dependence of the Inactivated Charge on Test Voltage*

The preferential charge inactivation observed here suggested a possible means of resolving the  $q_{\beta}$  and  $q_v$  contributions to the charge movement. For example, the subtraction shown in Fig. 4 *c* suggests that the  $q_v$  species could give rise to early events after membrane depolarization. This was now investigated over that selective range of test voltages where slow currents were most distinct. Test steps were

imposed 500 ms after application of a prepulse to  $-100$  mV from the holding potential. However, only two holding potentials were now used: either  $-100$  mV, at which the  $q_v$  charge would be intact, or  $-70$  mV, at which the  $q_v$  charge would be partially inactivated. Results were compared in the same fibers to enable comparisons to be drawn.

Fig. 6 A shows the isolated  $q_v$  charge movements at each test potential. These were deduced from the difference between test records obtained at the holding potential

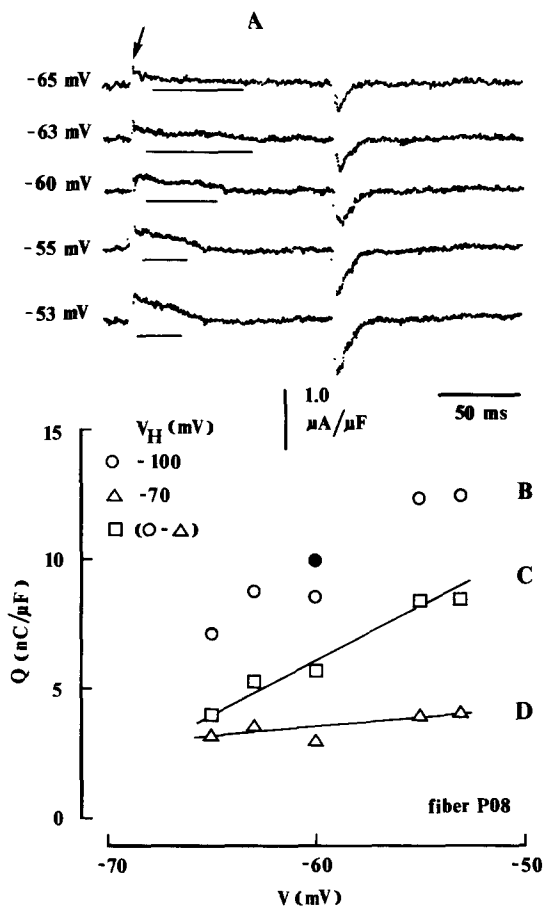


FIGURE 6. (A) The charge movement component obtained by comparing respective transients obtained in response to test voltage steps to a range of closely incremented membrane potentials,  $V$ , at holding potentials of  $-100$  and  $-70$  mV, respectively. Varying slow phases are emphasized by horizontal lines. Early charging currents are marked by the arrow. The charge-voltage,  $Q(V)$ , relationship of the inactivated  $q_v$  charge ( $C$ , squares) was obtained from the difference between  $B$  the  $Q(V)$  dependence at a holding voltage of  $-100$  mV (circles) and ( $D$ ) the corresponding  $Q(V)$  at a holding potential of  $-70$  mV (triangles). Lines were drawn by eye. The filled circle is a repeat reading after the holding voltage was returned to  $-100$  mV. Specific fiber cable constants:  $d = 92.34 \mu\text{m}$ ,  $R_m = 11.97 \text{ k}\Omega \text{ cm}^2$ ,  $C_m = 9.1 \mu\text{F}/\text{cm}^2$ . Fibers in EGTA-containing, low  $[\text{Ca}^{2+}]$  solutions in the absence of tetracaine.

of  $-100$  mV and those obtained at  $-70$  mV. The steady-state voltage dependence of the inactivated  $q_v$  charge (Fig. 6 C) was obtained by comparing results before (Fig. 6 B) and after (Fig. 6 D) the shifts in holding voltage. The various voltage dependences were distinct even in the limited range of test voltages examined. A measurement of nonlinear charge made at the end of the procedure when the holding voltage was returned to  $-100$  mV indicated that this charge inactivation was reversible (Fig. 6 B, filled symbol).

Delayed charge movements that extended over 50–70 ms were observed at the small depolarizations (Fig. 6*A*). In contrast, off  $q_v$  tails were relatively rapid simple decays (cf. Huang, 1984). The on  $q_v$  currents became considerably more rapid, with merger of the slow components even through the 10-mV range of test potentials explored. Furthermore, in all these cases, even in the presence of prolonged on currents, there was significant  $q_v$  charge movement early after imposition of the voltage steps (Fig. 6*A*, *arrow*). The  $q_v$  system, normally associated with late transfers of charge, therefore appears also to contribute early if not immediate capacity currents.

#### DISCUSSION

This paper examines the inactivation of  $q_b$  and  $q_v$  charge through sustained shifts in holding potential in intact amphibian muscle. Earlier reports described a voltage-dependent partial inactivation of the intramembrane charge in cut fibers under conditions of low extracellular  $[Ca^{2+}]$ . This coincided with an inhibition of intracellular calcium signals arising from excitation–contraction coupling. These observations suggested a functional parallel between charge and contractile activation (Brum et al., 1988*a, b*). This earlier study did not examine the individual components of the nonlinear charge that have been characterized in intact fibers (e.g., Adrian and Peres, 1979; Huang, 1981, 1988; Hui, 1983).

The experiments accordingly confirm the inactivation process for intact fibers and proceed to make the latter distinction, as this was of interest in elucidating functions of particular charge species. The first studies used large test pulses, as did the earlier work. Charge movements at such test potentials were simple monotonic decays and did not show discernible kinetic components. However, these experiments gave estimates of available steady-state charge. Distinctions between species were drawn on the basis of tetracaine sensitivity. In normal external  $[Ca^{2+}]$ , small shifts in holding voltage caused little charge inactivation. This contrasted with the gradual inactivation with cut fibers even under these conditions. In contrast, charge inactivation took place with even small voltage changes in reduced external  $[Ca^{2+}]$ . Charge movements thus are influenced by conditions of external  $Ca^{2+}$  in both cut and intact fibers and the effect is actually more pronounced in the latter preparation.

In contrast, tetracaine reduced available charge even in fully polarized fibers and to similar extents in the two solutions. Shifts in holding potential elicited little further inactivation and gave similar inactivation curves in either solution. The findings therefore attribute the voltage-dependent charge inactivation in low external  $[Ca^{2+}]$  to  $q_v$  (tetracaine-sensitive) charge.

The  $q_v$  charge has also been associated with slow (hump) currents, but these are observed only over a narrow potential range. A second series of experiments therefore applied smaller steps to such voltages. These showed that charge inactivation did not simply scale down the charging waveform; this is what would have been expected if the inactivation uniformly involved the charge as a whole. Instead, the inhibited current was distinct in form from the charge movement that remained. It included the delayed capacity current identified with the  $q_v$  charge. Furthermore,

similar procedures performed when tetracaine was present did not affect  $q_{\beta}$  charge movement.

Both kinds of experiments suggest that the parallel voltage-dependent inactivation of charge movement and of calcium signals arises primarily from influences on  $q_{\gamma}$  as opposed to  $q_{\beta}$  charge. Furthermore, the  $q_{\gamma}$  charge was implicated not only on the basis of its steady-state sensitivity to tetracaine, but also through the delayed transients it produces with smaller voltage steps. These findings complement an earlier report that also attributed a similar parallel inactivation due to nifedipine treatment to the  $q_{\gamma}$  system (Brum and Rios, 1987; Huang, 1990). Taken together these reinforce the possible relationship between the  $q_{\gamma}$  charge and the regulation of excitation–contraction coupling (Huang, 1981; Vergara and Caputo, 1982; Hui, 1983; Huang, 1988).

The preferential inactivation of  $q_{\gamma}$  charge under the conditions described here suggested a possible separation for their respective transients (Adrian and Peres, 1979; Huang, 1981; Hui, 1983; Adrian and Huang, 1984*a*). This would ideally extend to early times when the delayed  $q_{\gamma}$  and the  $q_{\beta}$  currents overlap, and to larger depolarizations when both produce rapid and consequently indistinguishable decays. A number of procedures have been developed for charge movement separation, each with particular problems and advantages. Adrian and Peres (1979) first inactivated the  $q_{\gamma}$  charge with large holding potential shifts in normal conditions of extracellular  $[Ca^{2+}]$ . However, this also inactivated  $\sim 50\%$  of the  $q_{\beta}$  charge (Huang, 1984). This precluded a full resolution of the individual contributions concerned through a comparison of records before and after the inactivation.

The conditions here inactivated the  $q_{\gamma}$  charge with relatively little effect on the  $q_{\beta}$  system. It could be obtained directly from data in a single intact fiber while avoiding changes in external solution or electrode impalement. It did not require assumed mathematical functions to fit the  $q_{\beta}$  or  $q_{\gamma}$  currents (Hui, 1983). It could therefore be useful where charging components could not be distinguished, but where pharmacological evidence nevertheless suggested multiple charge components. This applies to some amphibian preparations using cut fibers (Melzer et al., 1986; cf. Csernoch et al., 1988), and on occasion to mammalian muscle (Lamb, 1986; Hollingworth et al., 1990; cf. Hollingworth and Marshall, 1981; Simon and Beam, 1985). Differing results concerning the existence of  $q_{\gamma}$  charge in these different experimental systems might thus be resolved.

The separation here suggested early  $q_{\gamma}$  currents that began with, or at least soon after, the voltage step. These were demonstrated even with the delayed charging phases (humps). At any event, larger depolarizing steps reinforced this finding in eliciting considerably faster  $q_{\gamma}$  decays that became as rapid as the monotonic off tails. Thus, the  $q_{\gamma}$  charge, previously identified with slow currents, can contribute significant charge transfer even at early times.

The observations here thus reconcile evidence for the physiological role for  $q_{\gamma}$  charge with the results of dihydropyridine treatment (Rios and Brum, 1987; Huang, 1990) and extracellular cation withdrawal (Pizarro et al., 1989). The latter implicate early charging events in excitation–contraction coupling. The findings here also suggest that at least part of the  $q_{\gamma}$  current, the fraction that transfers early after the voltage steps, results from an independent mechanism, rather than from end events

in a reaction sequence (Horowicz and Schneider, 1981; Adrian and Huang, 1984b; Huang and Peachey, 1989). This has implications for hypotheses considering possible feed-forward or feedback roles in excitation–contraction coupling. However, this would not exclude the delayed portions of the charge transfers, where they occur, from being secondary to previous intramembrane events, or even to the  $\text{Ca}^{2+}$  release itself (Huang, 1981; Caille et al., 1985; Csernoch et al., 1989; Pizarro et al., 1990).

The author thanks Prof. R. H. Adrian for helpful discussions and Mr. W. Smith and Mr. M. Swann for skilled assistance. Dr. Judy Hughes of E. D. T. Analytical plc., Uxbridge, UK, provided useful advice on the assessment of  $\text{Ca}^{2+}$  activities and electrode calibration. Some of the equipment was provided by the Royal Society and by the Marmaduke Shield fund of Cambridge University.

*Original version received 21 June 1990 and accepted version received 25 February 1991.*

#### REFERENCES

- Adrian, R. H. 1978. Charge movement in the membrane of striated muscle. *Annual Reviews of Biophysics and Bioengineering*. 7:85–112.
- Adrian, R. H., and W. Almers. 1974. Membrane capacity measurements on frog skeletal muscle in media of low ionic content. *Journal of Physiology*. 237:573–605.
- Adrian, R. H., and W. Almers. 1976a. The voltage dependence of membrane capacity. *Journal of Physiology*. 254:317–338.
- Adrian, R. H., and W. Almers. 1976b. Charge movement in the membrane of striated muscle. *Journal of Physiology*. 254:339–360.
- Adrian, R. H., and C. L.-H. Huang. 1984a. Charge movements near the mechanical threshold in skeletal muscle of *Rana temporaria*. *Journal of Physiology*. 349:483–500.
- Adrian, R. H., and C. L.-H. Huang. 1984b. Experimental analysis of the relationship between charge movement components in skeletal muscle of *Rana temporaria*. *Journal of Physiology*. 353:419–434.
- Adrian, R. H., and A. Peres. 1979. Charge movement and membrane capacity in frog skeletal muscle. *Journal of Physiology*. 289:83–97.
- Adrian, R. H., and R. F. Rakowski. 1978. Reactivation of membrane charge movement and delayed potassium conductance in skeletal muscle fibres. *Journal of Physiology*. 278:533–557.
- Brum, G., R. Fitts, G. Pizarro, and E. Rios. 1988a. Voltage sensors of the frog skeletal muscle require calcium to function in excitation-contraction coupling. *Journal of Physiology*. 398:475–505.
- Brum, G., and E. Rios. 1987. Intramembrane charge movement in skeletal muscle fibres. Properties of charge 2. *Journal of Physiology*. 387:489–517.
- Brum, G., E. Rios, and E. Stefani. 1988b. Effects of extracellular calcium on calcium movement of excitation-contraction coupling in frog skeletal muscle fibres. *Journal of Physiology*. 398:441–473.
- Caille, J., M. Ildefonse, and O. Rougier. 1985. Excitation-contraction coupling in skeletal muscle. *Progress in Biophysics and Molecular Biology*. 46:185–239.
- Chandler, W. K., and C. S. Hui. 1990. Membrane capacitance in frog cut twitch fibers mounted in a double Vaseline-gap chamber. *Journal of General Physiology*. 96:225–256.
- Chandler, W. K., R. F. Rakowski, and M. F. Schneider. 1976. A non-linear voltage-dependent charge movement in frog skeletal muscle. *Journal of Physiology*. 254:243–283.
- Csernoch, L., C. L.-H. Huang, G. Szucs, and L. Kovacs. 1988. Differential effects of tetracaine on charge movements and  $\text{Ca}^{2+}$  signals in frog skeletal muscle. *Journal of General Physiology*. 92:601–612.
- Csernoch, L., I. Uribe, M. Rodriguez, G. Pizarro, and E. Rios. 1989.  $\text{Q}_r$  and calcium release flux in skeletal muscle fibers. *Biophysical Journal*. 55:88a. (Abstr.)

- Hodgkin, A. L., and S. Nakajima. 1972. The effects of diameter on the electrical constants of frog skeletal muscle fibres. *Journal of Physiology*. 221:105–120.
- Hollingworth, S., and M. W. Marshall. 1981. A comparative study of charge movement in frog skeletal muscle fibres. *Journal of Physiology*. 321:583–602.
- Hollingworth, S., M. W. Marshall, and E. Robson. 1990. The effect of tetracaine on charge movements in fast twitch rat skeletal muscle fibres. *Journal of Physiology*. 421:633–644.
- Horowicz, P. A., and M. F. Schneider. 1981. Membrane charge movement at contraction thresholds in skeletal muscle fibres. *Journal of Physiology*. 314:565–593.
- Huang, C. L.-H. 1981. Dielectric components of charge movements in skeletal muscle. *Journal of Physiology*. 313:187–205.
- Huang, C. L.-H. 1982. Pharmacological separation of charge movement components in frog skeletal muscle. *Journal of Physiology*. 324:375–387.
- Huang, C. L.-H. 1983. Time domain spectroscopy of the membrane capacitance in frog skeletal muscle. *Journal of Physiology*. 341:1–24.
- Huang, C. L.-H. 1984. Analysis of 'off' tails of intramembrane charge movements in skeletal muscle of *Rana temporaria*. *Journal of Physiology*. 356:375–390.
- Huang, C. L.-H. 1988. Intramembrane charge movements in skeletal muscle. *Physiological Reviews*. 68:1197–1247.
- Huang, C. L.-H. 1990. Voltage-dependent block of charge movement components by nifedipine in frog skeletal muscle. *Journal of General Physiology*. 96:535–558.
- Huang, C. L.-H., and L. D. Peachey. 1989. The anatomical localization of charge movement components in frog skeletal muscle. *Journal of General Physiology*. 93:565–584.
- Hui, C. S. 1983. Pharmacological studies of charge movements in frog skeletal muscle. *Journal of Physiology*. 337:509–529.
- Hui, C. S., and W. K. Chandler. 1990. Intramembrane charge movement in frog cut twitch fibers mounted in a double Vaseline-gap chamber. *Journal of General Physiology*. 96:257–297.
- Lamb, G. D. 1986. Components of charge movement in rabbit skeletal muscle: the effect of tetracaine and nifedipine. *Journal of Physiology*. 376:85–100.
- Melzer, W., M. F. Schneider, B. J. Simon, and G. Szucs. 1986. Intramembrane charge movement and calcium release in frog skeletal muscle. *Journal of Physiology*. 373:481–511.
- Pizarro, G., L. Csernoch, and E. Rios. 1990. An inward phase in intramembrane charge movement during a depolarizing pulse. *Biophysical Journal*. 57:341a. (Abstr.)
- Pizarro, G., R. Fitts, I. Uribe, and E. Rios. 1989. The voltage sensor of excitation-contraction coupling in skeletal muscle. Ion dependence and selectivity. *Journal of General Physiology*. 94:405–428.
- Rios, E., and G. Brum. 1987. Involvement of dihydropyridine receptors in excitation-contraction coupling in skeletal muscle. *Nature*. 325:717–720.
- Schneider, M. F., and W. K. Chandler. 1973. Voltage-dependent charge in skeletal muscle: a possible step in excitation-contraction coupling. *Nature*. 242:244–246.
- Sillen, L. G., and A. E. Martell. 1971. Stability Constants of Metal-Ion Complexes. The Chemical Society, London. 865 pp.
- Simon, B. J., and K. G. Beam. 1985. Slow charge movement in mammalian skeletal muscle. *Journal of General Physiology*. 85:1–19.
- Vergara, J., and C. Caputo. 1982. Effects of tetracaine on charge movements and calcium signals in frog skeletal muscle. *Proceedings of the National Academy of Sciences, USA*. 80:1477–1481.